Kinetics of the CCO + NO and CCO + NO_2 Reactions

W. David Thweatt, Mark A. Erickson, and John F. Hershberger*

Department of Chemistry, North Dakota State University, Fargo, North Dakota 58105

Received: March 31, 2003; In Final Form: September 16, 2003

The kinetics of the reaction of CCO radicals with NO and NO_2 were studied using time-resolved infrared diode laser absorption spectroscopy. The rate constants were determined to be $k_{CCO+NO} = (5.36 \pm 0.5) \times 10^{-11}$ and $k_{CCO+NO_2} = (6.89 \pm 0.5) \times 10^{-11}$ cm^3 molecule^{-1} s^{-1} at 298 K. These rate constants have virtually no temperature dependence over the range 298−573 K, with Arrhenius fits given by $k_{CCO+NO} = (1.66 \pm 0.5) \times 10^{-10} \exp[(-337 \pm 100)/T]$ and $k_{CCO+NO_2} = (8.51 \pm 1.5) \times 10^{-11} \exp[(-63 \pm 80)/T]$ (error bars represent one standard deviation). Product channel measurements were performed on the CCO + NO reaction. After consideration of secondary chemistry, we obtain the branching ratios $\phi(CN + CO_2) = 0.13 \pm 0.05$ and $\phi(CO + NCO) = 0.87 \pm 0.05$ at 298 K. Ab initio quantum chemical calculations at the QCISD(T)/6-311G(2df,2pd) level of theory were used to examine probable reaction pathways.

Introduction

Reactions between small molecular radicals and nitrogen oxides are crucial elementary steps in models of NO_x formation and removal in combustion systems.[1] One such species of interest in combustion kinetics is the CCO radical. This molecule has been the subject of several spectroscopic investigations.[2−7] Only a few reports of kinetic measurements of CCO reactions have appeared, however.[8,9] For the CCO + NO reaction, there is one previous direct measurement; Donnelly et al. used 266 nm laser photolysis of C_3O_2 and laser-induced fluorescence detection to obtain $k = (4.33 \pm 0.12) \times 10^{-11}$ cm^3 molecule^{-1} s^{-1} at 298 K.[9] An older relative rate measurement has also been reported.[10] No information on product channels is available, and no reports of the CCO + NO_2 reaction have appeared.

In this study, we report infrared diode laser measurements of both the total rate constants (over the temperature range 298−573 K) and the product branching ratios (at 298 K) of the CCO + NO reaction. Ab initio calculations of the potential energy surface of this reaction are also reported, and are useful in the interpretation of isotopic labeling experiments used to determine the branching ratio. In addition, we report rate constant measurements of the CCO + NO_2 reaction.

The title reactions may produce several products. For CCO + NO, only two are exothermic:

$$CCO + NO \rightarrow CO_2 + CN \quad \Delta H_{298} = -335 \text{ kJ/mol} \quad (1a)$$

$$\rightarrow CO + NCO \quad \Delta H_{298} = -328 \text{ kJ/mol} \quad (1b)$$

$$\rightarrow C_2 + NO_2 \quad \Delta H_{298} = 494 \text{ kJ/mol} \quad (1c)$$

$$\rightarrow CNC + O_2 \quad \Delta H_{298} = 179 \text{ kJ/mol} \quad (1d)$$

$$\rightarrow CCN + O_2 \quad \Delta H_{298} = 182 \text{ kJ/mol} \quad (1e)$$

$$CCO + NO_2 \rightarrow CN + CO + O_2 \quad \Delta H_{298} = 4.9 \text{ kJ/mol} \quad (2a)$$

$$\rightarrow CO_2 + NCO \quad \Delta H_{298} = -585.5 \text{ kJ/mol} \quad (2b)$$

$$\rightarrow NCCO + O_2 \quad (2c)$$

The thermochemical information for reactions (1a−d) and (2a−b) is obtained from standard tables,[11] except for ΔH_f of NCO, which was obtained from recent measurements.[12] Since channels (1c), (1d), and (1e) are endothermic, they cannot be significant product channels at moderate temperatures and are not considered further in this study. The most important secondary reaction in the CCO + NO system is that of NCO produced in reaction 1b with NO:

$$NCO + NO \rightarrow CO + N_2O \quad (3a)$$

$$\rightarrow N_2 + CO_2 \quad (3b)$$

The kinetics of this reaction have been extensively studied.[13−18] At 298 K, $k_3 = 3.2 \times 10^{-11}$ cm^3 molecule^{-1} s^{-1},[13−17] and the branching ratios are $\phi_{3a} = 0.44 \pm 0.07$ and $\phi_{3b} = 0.56 \pm 0.07$.[18]

CCO radicals were formed in our experiments using photolysis of carbon suboxide (C_3O_2). The photodissociation dynamics of C_3O_2 has been previously studied by Anderson and Rosenfeld.[19] They suggest that at 193 nm, the primary photoproducts are ground-state CO and excited-state CCO ($a^1\Delta$); however, at 248 nm, mostly ground-state CCO ($X^3\Sigma^-$) is formed. Most of the experiments reported here used 266 nm photolysis in order to minimize the formation of excited-state CCO molecules.

Experimental Section

The time-resolved infrared diode laser technique has been described previously.[18,20] Continuous, high-resolution (0.0003 cm^{-1}) infrared radiation from a lead-salt diode laser (Laser Photonics) was made collinear with 266-nm radiation from an Nd:YAG laser (Lumonics) by means of a dichroic mirror. The laser beams were then copropagated down a 1.43-m Pyrex absorption cell. The infrared light then passed through a 0.25-m monochromator and was focused onto an InSb detector (Cincinnati Electronics, ~1 μs response). Transient signals were collected and averaged on a digital oscilloscope and stored on a computer. The HITRAN database[21] and published spectral data[2] for CCO were used as an aid in calibrating laser wavelengths and identifying transitions.

Carbon suboxide was prepared just prior to each experiment by reaction of phosphorus pentoxide (P_2O_5) (Aldrich) with

* Corresponding author. E-mail: john.hershberger@ndsu.nodak.edu.

10.1021/jp0304125 CCC: $27.50
Published on Web 12/04/2003

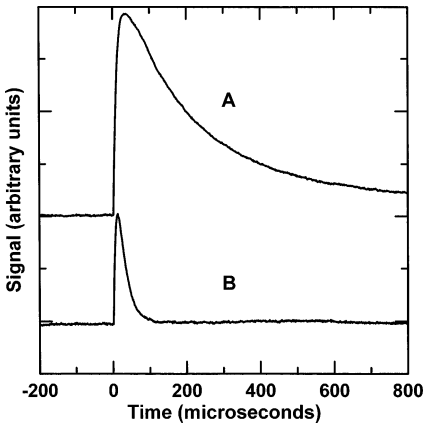

Figure 1. Transient infrared absorption signal of CCO at 1984.326 cm^{-1}, produced by 266 nm photolysis of C_3O_2. Reaction conditions: $P_{C_3O_2}$ = 0.500 Torr, P_{NO} = 0.0 Torr (trace A), 0.060 Torr (trace B), P_{SF_6} = 1.00 Torr, P_{Xe} = 1.00 Torr, T = 298 K.

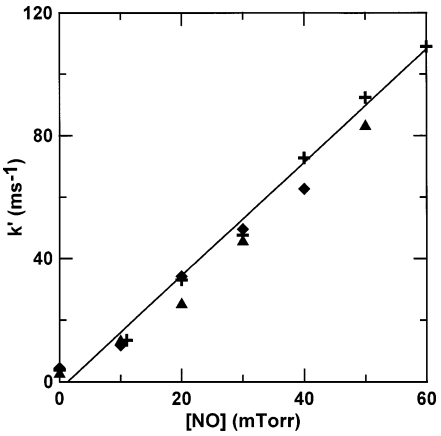

Figure 2. Pseudo-first-order decay rate constant of CCO radical as a function of NO pressure. Reaction conditions: $P_{C_3O_2}$ = 0.500 Torr, P_{NO} = variable, P_{SF_6} = 1.00 Torr, P_{Xe} = 1.00 Torr. Crosses: 298 K. Diamonds: 378 K. Triangles: 573 K.

malonic acid (Aldrich) as described in the literature.[22] The resulting gas was then passed slowly through a U-tube filled with $Ca(OH)_2$ several times, then frozen at 77 K into a 500 mL Pyrex storage bulb. The resulting gas mixture is usually at least 60% CO_2 due to competing thermal decarboxylation reactions. Other reagents were obtained from Matheson and purified by several freeze−pump−thaw cycles. Typical reaction conditions were 0.1−0.5 Torr C_3O_2 sample, 0.050−0.80 Torr NO or NO_2, 1.0 Torr SF_6, and 1.0 Torr Xe. Upon introduction into the reaction cell, gases were allowed to stand ∼5 min in order to ensure complete mixing.

The following transitions were probed:

CCO R(18) line (ν_1 vibrational band) at 1984.326 cm^{-1}

CN $\upsilon = 0$, R(12) line at 2085.043 cm^{-1}

N_2O (000) P(14) line at 2211.398 cm^{-1}

$C^{16}O$ $\upsilon = 0$, P(10) line at 2103.270 cm^{-1}

$C^{18}O$ $\upsilon = 0$, R(2) line at 2102.9117 cm^{-1}

$^{18}O^{12}C^{18}O$ (000) R(14) line at 2323.798 cm^{-1}

$^{16}O^{12}C^{18}O$ (000) P(11) line at 2323.694 cm^{-1}

Results and Discussion

Total Rate Constant Measurements. Figure 1 shows a typical transient signal for CCO detection at 1984.326 cm^{-1}. As shown, the signals display a rise time of ∼35 μs followed by a slow decay. This suggests that most of the nascent CCO is produced in excited vibrational and/or electronic states, and the rise time is indicative of the rate of relaxation into the probed ground state. The buffer gases included in the reaction mixture were necessary to ensure that this relaxation occurred on a time scale relatively short compared to the subsequent reaction. SF_6 is an efficient collision partner for the vibrational relaxation of many triatomic molecules,[23,24] and xenon is expected to promote the spin-forbidden process:

$$CCO\ (a^1\Delta) + Xe \rightarrow CCO\ (X^3\Sigma^-) + Xe$$

Experiments performed without Xe buffer gas yielded signals similar in shape to those of Figure 1, but substantially smaller in magnitude. This suggests that some excited electronic state CCO is produced even at our photolysis wavelength of 266 nm, which is somewhat contradictory to the suggestion of Anderson and Rosenfeld that primarily ground electronic state CCO is produced at the nearby 248 nm wavelength.[19] We did perform a few experiments using 193 nm photolysis wavelengths, but found rise times substantially slower than those in Figure 1. As a result, most of the experiments reported here used 266 nm.

As shown in Figure 1, addition of NO significantly increased the rate of decay of the transient signals, indicating reactive removal of CCO by reactions (1) or (2). In principle, a fit of the decay portion of the signal to an exponential function would yield the pseudo-first-order rate constant k'. This approach assumes, however, that the rise rates in the signal are very fast compared to the decay rates. Some of our signals, especially at high [NO], have decay rates that approach the rise rates. As a result, the transient signals were fit to a function consisting of the sum of a rising exponential and a decaying exponential, using a nonlinear Marquardt algorithm. This procedure yields decay rates that are typically ∼10% greater than those obtained from a single decaying exponential fit. The decay rate is then interpreted as the pseudo-first-order rate constant k'. As per standard pseudo-first-order kinetics, a plot of k' as a function of [NO] yields a straight line given by

$$k' = k_1[NO] + k_d$$

where k_d is the decay rate in the absence of NO (due to reaction of CCO with itself, the precursor, or diffusion of CCO radicals out of the probed reaction zone). k_1 is the desired bimolecular rate constant, obtained from the slope of the k' vs [NO] plot. Figure 2 shows such a plot at several reaction temperatures for the CCO + NO reaction. Figure 3 shows a similar treatment for the CCO + NO_2 reaction. Figure 4 shows Arrhenius plots for the two reactions. Both reactions have nearly temperature-independent rate constants over the range 298−573 K. The data were fit to the following Arrhenius expressions:

$$k_1(CCO + NO) = (1.66 \pm 0.5) \times 10^{-10} \exp[(-337 \pm 100)/T]$$

$$k_2(CCO + NO_2) = (8.51 \pm 1.5) \times 10^{-11} \exp[(-63 \pm 80)/T]$$

At 298 K, the rate constants are $k_1 = (5.36 \pm 0.5) \times 10^{-11}$ and $k_2 = (6.89 \pm 0.5) \times 10^{-11}$ cm^3 $molecule^{-1}$ s^{-1}. One previous direct study reported a somewhat lower value of $k_1 = (4.33 \pm 0.12) \times 10^{-11}$ cm^3 $molecule^{-1}$ s^{-1} at 298 K,[9] using LIF detection of CCO. Our work represents the first reported value of k_2.

Product Channel Measurements. All of the reactants and products in channels (1a) and (1b) may in principle be detected

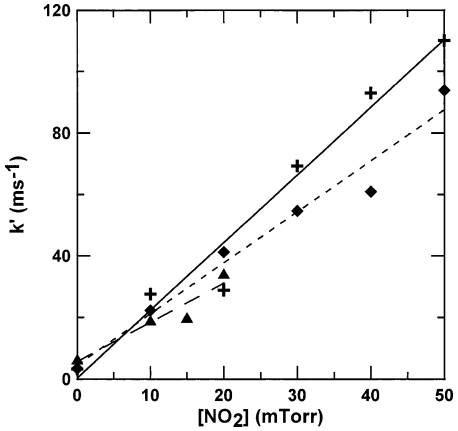

Figure 3. Pseudo-first-order decay rate constant of CCO radical as a function of NO_2 pressure. Reaction conditions: $P_{C_3O_2} = 0.500$ Torr, P_{NO_2} = variable, $P_{SF_6} = 1.00$ Torr, $P_{Xe} = 1.00$ Torr. Crosses: 298 K. Diamonds: 378 K. Triangles: 573 K.

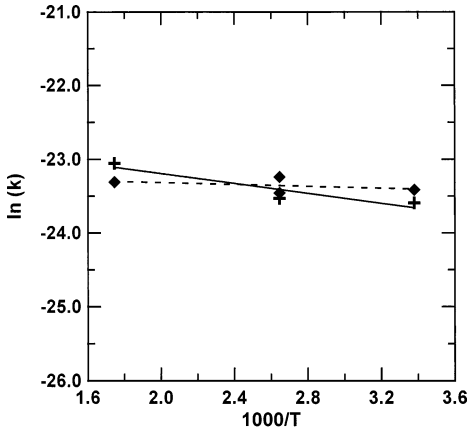

Figure 4. Arrhenius plots for the CCO + NO (crosses) and CCO + NO_2 (diamonds) reactions.

by infrared absorption spectroscopy. The nontransient species CO and CO_2 are the easiest to quantify. It may therefore appear that ϕ_{1a} and ϕ_{1b} may be readily obtained by quantifying the yields of these products. Unfortunately, several sources of background signals complicate this approach. First, CO_2 is present as a significant impurity in the C_3O_2 samples. Attempts to remove CO_2 by flowing the sample through an Ascarite trap were unsuccessful, apparently resulting in decomposition of the C_3O_2. We note that even a few percent impurity will significantly interfere with any attempt to detect $^{16}O^{12}C^{16}O$ reaction products. Isotopic substitution of reagents is therefore an absolute necessity in order to quantify the CO_2 yield. Detection of CO is also problematic, because it is formed in the photolysis (presumably with unity quantum yield). As a result, a large transient signal for CO was observed upon the photolysis of a C_3O_2/buffer gas mixture, without any NO reagent. If NO is included in the reaction mixture, additional CO formation routes (1b) and the secondary reaction (3a) are available. We therefore expected the CO yield to be substantially increased when NO was included. In fact, no such increase was observed; the CO yield was found to be essentially unchanged over the range 0−0.5 Torr NO. Our explanation of this is that even in the absence of nitric oxide reagent, CCO can undergo reactions, either with itself or with C_3O_2, ultimately resulting in the formation of CO. It is therefore difficult to determine how much of the observed CO originated from channel (1b).

Attempts were made to detect CN radicals produced in channel (1a). No transient signals were found, suggesting that

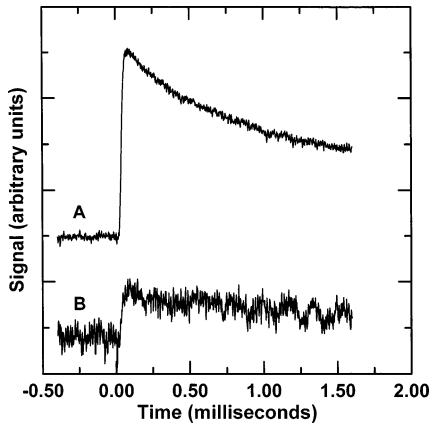

Figure 5. Transient infrared absorption signals of $^{18}O^{12}C^{18}O$ (000) R(14) at 2323.798 cm^{-1} (trace A) and $^{18}O^{12}C^{16}O$ (000) P(11) at 2323.694 cm^{-1} (trace B). Reaction conditions: $P_{C_3O_2} = 0.100$ Torr, $P_{NO} = 0.200$ Torr, $P_{SF_6} = 1.00$ Torr, $P_{Xe} = 1.00$ Torr, $T = 298$ K.

(1a) is a minor product channel. CO_2 detection by infrared spectroscopy is much more sensitive than CN detection, however, so the experiments described below give a much better estimate of the importance of channel (1a).

The following approach was found to provide the most reliable estimate of the product branching ratio of reaction (1). CCO was allowed to react with isotopically labeled $N^{18}O$:

$$CCO + N^{18}O \rightarrow CN + {}^{16}O^{12}C^{18}O \quad (1a)$$

$$\rightarrow C^{16}O + NC^{18}O \quad (1b)$$

The secondary reaction (3) then produces doubly labeled CO_2:

$$NC^{18}O + N^{18}O \rightarrow C^{18}O + N_2{}^{18}O \quad (3a)$$

$$\rightarrow N_2 + {}^{18}O^{12}C^{18}O \quad (3b)$$

Because we know the branching ratio of reaction (3), i.e., $\phi_{3b} = 0.56$, one can obtain the yield of channel (1b) by measuring $[^{18}O^{12}C^{18}O]$, if $[N^{18}O]$ is sufficiently high to ensure that every $NC^{18}O$ radical reacts with $N^{18}O$:

$$[NC^{18}O] = [{}^{18}O^{12}C^{18}O]/0.56$$

Measurement of $[^{16}O^{12}C^{18}O]$ provides a direct measurement of the yield of channel (1a). Comparison of $[^{16}O^{12}C^{18}O]$ and $[NC^{18}O]$ then yields the branching ratios ϕ_{1a} and ϕ_{1b}. This procedure thus separately measures the CO_2 yield produced by the direct reaction (1a) from that produced by the secondary chemistry, channel (3b), without undue interference from the unlabeled CO_2 impurity present in the C_3O_2 sample.

The procedure just described relies on the crucial assumption that in channel (1b), the 18-labeled oxygen from the NO reactant ends up on the NCO and not the CO product. Ab initio computations, described below, strongly suggest that this assumption is valid.

Figure 5 shows transient signals for the singly and doubly labeled isotopes of CO_2 upon photolysis of $C_3O_2/{}^{15}N^{18}O/SF_6$/Xe mixtures. ($^{15}N^{18}O$ was used because it was readily available; the nitrogen labeling is irrelevant in this experiment). The $^{18}O^{12}C^{18}O$ trace is an average of 10 shots, and the $^{16}O^{12}C^{18}O$ is an average of 40 shots. The signal for $[^{16}O^{12}C^{18}O]$ is somewhat noisy because the CO_2 impurity in the C_3O_2 sample has a small but nonzero natural abundance of this isotope, resulting in a significant but manageable level of static background. The peak amplitudes of the transient signals were converted into absolute

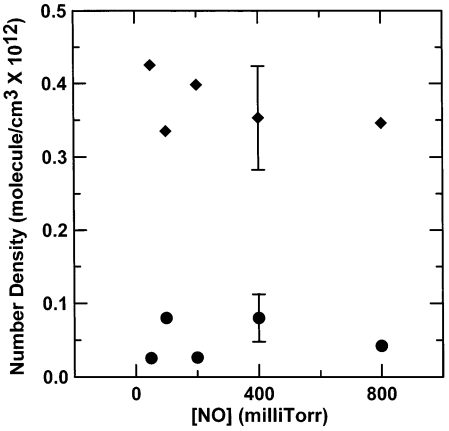

Figure 6. $^{18}O^{12}C^{18}O$ (diamonds) and $^{16}O^{12}C^{18}O$ (circles) product yields as a function of $N^{18}O$ pressure. Reaction conditions: $P_{C_3O_2} = 0.100$ Torr, P_{NO} = variable, $P_{SF_6} = 1.00$ Torr, $P_{Xe} = 1.00$ Torr, $T = 298$ K.

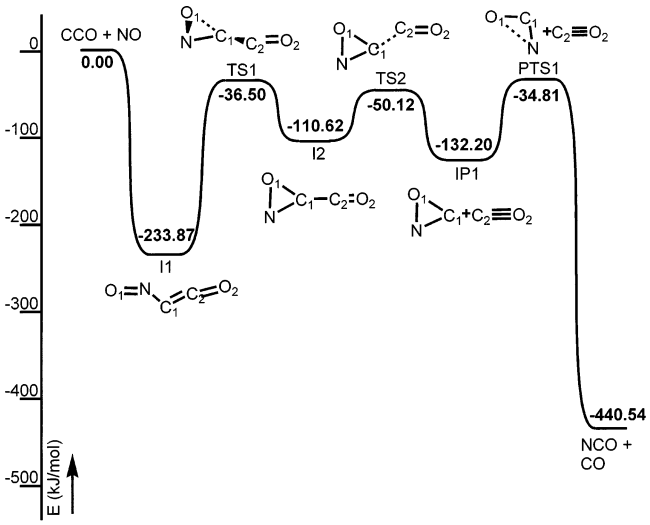

Figure 7. A portion of the QCISD(T)/6-311G(2df,2pd)//MP2/6-31G* potential energy surface of CCO + NO: a reaction path producing CO + NCO.

number densities using formulas previously described. One modification to that procedure was necessary: since HITRAN assumes natural isotopic abundances, linestrengths from the database were modified by dividing by the natural abundance of the detected isotope (0.0039 for singly labeled, 4×10^{-6} for doubly labeled). Figure 6 shows the resulting product yields as a function of NO pressures. The product yields and branching ratios were found to be essentially independent of NO pressure over the range 0.05−0.8 Torr. The average of 18 experiments over this pressure range gives the following results: $\phi_{1b}/\phi_{1a} = 6.69 \pm 2.0$. If we assume that only channels (1a) and (1b) contribute, we obtain the absolute branching ratios $\phi_{1a} = 0.13 \pm 0.05$ and $\phi_{1b} = 0.87 \pm 0.05$, where the error bars represent one standard deviation.

In principle, the formation of vibrationally and/or electronically excited radicals in the photolysis step can affect product yield determinations. As Figure 1 shows, at low NO pressures (∼0.05−0.1 Torr), the rate of reaction with NO (the decay rate) is somewhat slower than the rate of relaxation of CCO into the ground vibrational and electronic state. Under these conditions, the CCO + NO reaction therefore predominates over excited-state CCO* + NO reaction events. At higher NO pressures (not shown in Figure 1), the rate of reaction with NO is presumably faster than the relaxation rate (which is primarily governed by collisions with buffer gas molecules), so CCO* + NO reactions

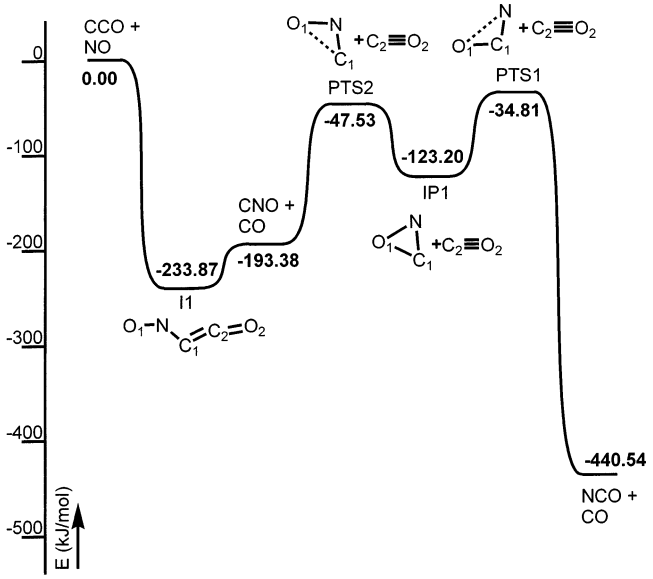

Figure 8. Another reaction path producing CO + NCO. Calculation at same level of theory as Figure 7.

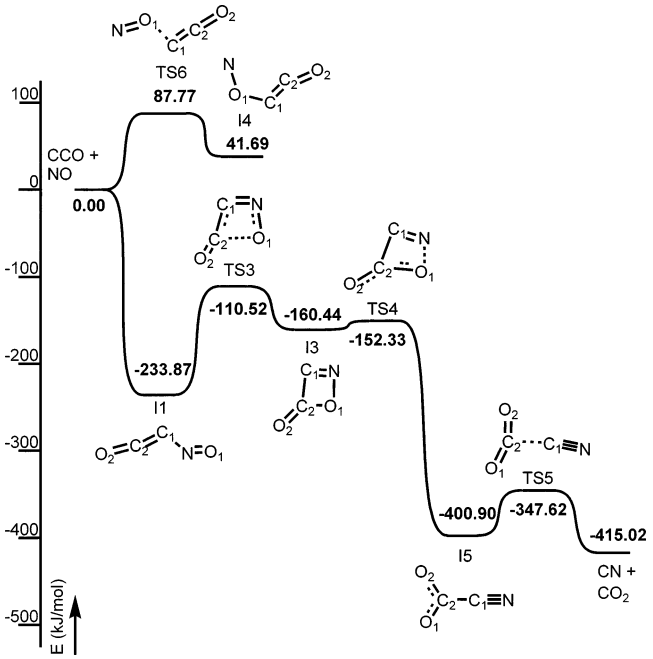

Figure 9. A reaction path producing CN + CO_2. Calculation at same level of theory as Figure 7. Also shown is part of a high energy pathway involving an NOCCO structure (see text).

become more important. The observation in Figure 6 of constant product yields over the range 0.05−0.8 Torr of NO suggests, however, that this competition between ground- and excited-state reactions does not significantly affect our results, probably because the product yields of excited-state reaction with NO are similar to those of ground-state reactions.

Donnelly et al. suggested that a dark reaction between C_3O_2 and NO may have occurred in their experiments, as evidenced by a slow pressure rise upon mixing of the reagents, as well as their observation of otherwise unexplained fluorescence signals upon 266-nm excitation of C_3O_2/NO. We did not observe any pressure increases in our experiments, but a slow secondary reaction between C_3O_2 and NO could result in some depletion of reagents. Depletion of C_3O_2 would merely reduce the initial CCO radical concentration, without affecting the pseudo-first-order kinetics or branching ratio measurements. Loss of NO,

TABLE 1: Ab Initio Calculations of Reactants and Products[a]

species	CCO	NO	CO2	CO	CN	NCO
2S+1	3	2	1	1	2	2
symmetry	$C_{\infty v}$	$C_{\infty v}$	$D_{\infty h}$	$C_{\infty v}$	$C_{\infty v}$	$C_{\infty v}$
$R(C_1-C_2)$	1.379					
$R(C_2-O_1)$			1.180			
$R(C_2-O_2)$	1.173		1.180	1.151		
$R(N-O_1)$		1.143				
$R(C_1-N)$					1.136	1.255
$R(C_1-O_1)$						1.167

[a] Bond lengths in Angstroms, angles in degrees.

TABLE 2: Ab Initio Calculations of Intermediates[a]

species	I1	I2	I3	I4	I5	IP1
2S+1	2	2	2	2	2	2
symmetry	C_s	C_1	C_s	C_s	C_{2v}	C_s
$R(O_1-N)$	1.195	1.442	1.512	1.316		1.433
$R(N-C_1)$	1.273	1.375	1.216		1.161	1.360
$R(C_1-C_2)$	1.352	1.294	1.592	1.367	1.460	
$R(C_2-O_2)$	1.164	1.146	1.179	1.171	1.254	
$R(C_2-O_1)$					1.254	
$R(O_1-C_1)$				1.351		1.384
$A(O_1-N-C_1)$	138.6	62.0	92.9			63.5
$A(N-C_1-C_2)$	112.4	102.8	93.4		180.0	57.5
$A(C_1-C_2-O_2)$	168.4	130.0	142.0	160.2	122.4	
$A(N-O_1-C_1)$				121.0		
$A(O_1-C_1-C_2)$				121.7	122.4	
$A(O_1-C_2-O_2)$					115.2	
$D(O_1-N-C_1-C_2)$	180.0	134.9	0.0		0.0	
$D(N-C_1-C_2-O_2)$	0.0	163.4	180.0			
$D(N-O_1-C_1-C_2)$				0.0		
$D(O_1-C_1-C_2-O_2)$				180.0		

[a] Bond lengths in Angstroms, angles in degrees.

however, would cause a systematic error in the total rate constant determinations. To test for this possibility, we tuned the diode laser to weak NO transitions near 1900 cm^{-1} to monitor [NO] over a ~1 h time scale upon mixing of reagents. Only a very slight loss of NO was observed, and was insignificant over the 5−10 min time scale of our measurements. This suggests that dark reactions, if any, occur too slowly to affect our data.

Ab Initio Calculations. To better understand the reaction mechanism, and to help interpret the branching ratio experiments, ab initio quantum chemical calculations were performed on the doublet reaction surface. Unless otherwise noted, the geometries were calculated using the MP2 method[25] with Pople's 6-31G* basis set[26] (MP2/6-31G*). Stationary points (minima and transition states) were confirmed with vibrational analysis. Zero-point vibrational energy corrections were calculated at the Hartree−Fock[27] level of theory with the same basis set, then scaled by a factor of 0.8978.[28] Absolute electronic energies were calculated at the MP2/6-31G* geometry using quadratic configuration interaction with singles, doubles, and perturbative triples excitations[29] with Pople's 6-311G(2df,2pd) basis set[30] (QCISD(T)/6-311G(2df,2pd)). In two cases (I5 and TS5), due to massive MP2 spin-contamination problems, transition-state geometries were refined at the B3LYP/6-31G* and B3LYP/6-311G* levels of theory,[31,32] respectively. All ab initio quantum chemical calculations were performed on IBM RS6000 3CT machines using Gaussian 94, version E.[33]

Figures 7, 8, and 9 show important stationary points along the calculated minimum energy pathways on the ground-state doublet PES. As shown, N → C attack can produce a bent ONCCO complex (I1) which lies 234 kJ/mol below the reactants. Several possible pathways from I1 exist. One route (Figure 7) involves formation of an (NOC)CO (three-membered ring) structure (I2), followed by C−C bond fission to produce CO and a cyclic (ONC) structure (IP1). Opening of the three-membered ring can then produce the NCO + CO product channel. Alternatively, as shown in Figure 8, the bent ONCCO complex (I1) could dissociate directly to CNO + CO, and the CNO then may have enough energy to isomerize, via structure IP1, to NCO. Channel (1a) is accessible by a route shown in Figure 9, involving formation of a four-membered NOCCO structure (I3), followed by a ring-opening N−O bond fission to structure I5, and subsequent C−C bond fission to CN + CO_2. These pathways are all energetically accessible from the CCO + NO starting energy, and if $N^{18}O$ is used, the labeled oxygen would end up on the NCO product in (1b), rather than CO. This is therefore consistent with the assumption used to interpret our isotopic labeling experiments. The most obvious reaction path that would violate this assumption is also shown in Figure 9, and would involve formation of an NOCCO intermediate (I4), which could then rearrange via a four-membered ring (not shown), followed by N−O and C−C bond fission to form NCO + CO products. If this pathway were active, CCO + $N^{18}O$

TABLE 3: Ab Initio Calculations of Transition States[a]

species	TS1	TS2	TS3	TS4	TS5	TS6	PTS1	PTS2
2S+1	2	2	2	2	2	2	2	2
symmetry	C_1	C_1	C_S	C_S	C_S	C_S	C_S	C_S
$R(O_1-N)$	1.330	1.425	1.366	1.513		1.180	2.253	1.316
$R(N-C_1)$	1.352	1.374	1.295	1.216	1.162		1.438	1.438
$R(C_1-C_2)$	1.390	1.917	1.458	1.593	1.926	1.385		
$R(C_2-O_2)$	1.156	1.146	1.134	1.179	1.211	1.172	1.151	1.151
$R(C_2-O_1)$					1.163			
$R(O_1-C_1)$						1.836	1.402	2.250
$A(O_1-N-C_1)$	78.2	62.0	98.8	92.9			36.9	109.5
$A(N-C_1-C_2)$	134.2	102.8	105.3	93.4	171.3			
$A(C_1-C_2-O_2)$	146.3	130.3	151.4	142.0	88.1	172.6		
$A(N-O_1-C_1)$						122.2		
$A(O_1-C_1-C_2)$						96.8		
$A(O_1-C_2-O_2)$					157.9			
$D(O_1-N-C_1-C_2)$	89.7	134.9	0.0	0.0				
$D(N-C_1-C_2-O_2)$	171.0	163.4	180.0	180.0				
$D(N-O_1-C_1-C_2)$					180.0	180.0		
$D(O_1-C_1-C_2-O_2)$					180.0	180.0		

[a] Bond lengths in Angstroms, angles in degrees.

would produce NCO + $C^{18}O$, in contrast to our assumptions. The most important result from the ab initio calculations is that the NOCCO structure is endoergic by 42 kJ/mol relative to the CCO + NO reactants. Furthermore, the most direct path to this structure, via TS6, involves a 88 kJ/mol barrier. Although other pathways (not calculated) to I4 may exist (for example, opening of the NOCCO three-membered ring (I2) via N−C bond fission), the NOCCO structure itself is sufficiently high in energy to exclude these pathways as major contributors to the reaction mechanism.

One limitation of both the calculations and the experiments reported above is that we cannot rule out the possibility that a major product is the high energy isomer CNO rather than NCO. We have no direct method of detecting CNO, however the following experiment was performed. We measured the N_2O yield using natural abundance samples, and the $^{18}O^{12}C^{18}O$ yield using $N^{18}O$ labeling. Since these products are formed only in reactions (3a) and (3b), the ratio of these product yields should be the same as previously measured branching ratios of reaction (3). We obtain $\phi_{3a} = 0.49 \pm 0.02$ and $\phi_{3b} = 0.51 \pm 0.02$, in reasonable agreement with our previous measurements of $\phi_{3a} = 0.44$ and $\phi_{3b} = 0.56$.[18] This strongly suggests one of the following: either the (NCO) product formed in the title reaction is NCO and not CNO, or any CNO quickly rearranges to NCO, or that the CNO + NO reaction (for which no literature data exist) has branching ratios similar to NCO + NO.

Conclusions

The kinetics of the CCO + NO and CCO + NO_2 reactions were investigated. Both reactions are fast, with nearly temperature-independent rate constants. Product yield experiments using isotopically labeled NO combined with ab initio calculations demonstrate that NCO + CO is the major product channel of the CCO + NO reaction at 298 K, with a branching ratio of 0.87 ± 0.05. CN + CO_2 is a minor channel, with a branching ratio of 0.13 ± 0.05.

Acknowledgment. This work was supported by the Division of Chemical Sciences, Office of Basic Energy Sciences of the Department of Energy, Grant DE-FG03-96ER14645.

References and Notes

(1) Miller, J. A.; Bowman, C. T. *Prog. Energy Combust. Sci*. **1989**, *15*, 287.
(2) Yamada, C.; Kanamori, H.; Horiguchi, H.; Tsuchiya, S.; Hirota, E. *J. Chem. Phys.* **1986**, *84*, 2573.
(3) Moazzen-Ahmadi, N.; Boere, R. T. *J. Chem. Phys.* **1999**, *110*, 955.
(4) Moazzen-Ahmadi, N.; Boere, R. T. *J. Chem. Phys.* **1998**, *108*, 6588.
(5) Ohashi, N.; Kiryu, R.; Okino, S.; Fujitake, M. *J. Mol. Spectrosc.* **1993**, *157*, 50.
(6) Fujitake, M.; Kiryu, R.; Ohashi, N. *J. Mol. Spectrosc*. **1992**, *154*, 169.
(7) Becker, K. H.; Horie, O.; Schmidt, V. H.; Wiesen, P. *Chem. Phys. Lett*. **1982**, *90*, 64.
(8) Bauer, W.; Becker, K. H.; Meuser R. *Ber. Bunsen-Ges. Phys. Chem.* **1985**, *89*, 340.
(9) Donnelly, V. M.; Pitts, W. M.; McDonald, J. R. *Chem. Phys.* **1980**, *49*, 289.
(10) Williamson, D. G.; Bayes, K. D. *J. Am. Chem. Soc.* **1967**, *89*, 3390.
(11) Chase, M. W., Jr. *J. Phys. Chem. Ref. Data*, Monograph No. 9, NIST-JANAF Thermochemical Tables, 4th ed.; 1998.
(12) Cyr, D. R.; Continetti, R. E.; Metz, R. B.; Osborn, D. L.; Neumark, D. M. *J. Chem. Phys.* **1992**, *97*, 4937.
(13) Perry, R. A. *J. Chem. Phys*. **1985**, *82*, 5485.
(14) Hancock, G.; McKendrick, K. G. *Chem. Phys. Lett.* **1986**, *127*, 125.
(15) Atakan, B.; Wolfrum, J. *Chem. Phys. Lett*. **1991**, *178*, 157.
(16) Mertens, J. D.; Dean, A. J.; Hanson, R. K.; Bowman, C. T. *Symp. (Int.) Combust. Proc*. **1992**, *24*, 701.
(17) Juang, D. Y.; Lee, J.-S.; Wang, N. S. *Int. J. Chem. Kinet.* **1995**, *27*, 1111.
(18) Cooper, W. F.; Park, J.; Hershberger, J. F. *J. Phys. Chem*. **1993**, *97*, 3283.
(19) Anderson, D. J.; Rosenfeld, R. N. *J. Chem. Phys*. **1991**, *94*, 7857.
(20) Quandt, R. W.; Hershberger, J. F. *J. Phys. Chem*. **1996**, *100*, 9407.
(21) Rothman, L. S.; Gamache, R. R.; Tipping, R. H.; Rinsland, C. P.; Smith, M. A. H.; Benner, D. C.; Devi, V. M.; Flaud, J. M.; Camy-Peyret, C.; Perrin, A.; Goldman, A.; Massie, S. T.; Brown, L. R.; Toth, R. A. *J. Quant. Spectrosc. Radiat. Transfer* **1992**, *48*, 469.
(22) Long, D. A.; Murfin, F. S.; Williams, R. L. *Proc. R. Soc. London Ser. A* **1954**, *223*, 251.
(23) Fakhr, A.; Bates, R. D., Jr. *Chem. Phys. Lett*. **1980**, *71*, 381.
(24) Stephenson, J. C.; Moore, C. B. *J. Chem. Phys.* **1970**, *52*, 2333.
(25) Krishnan, R.; Pople, J. A. *Int. J. Quantum Chem.* **1978**, *14*, 91.
(26) Hehre, W. J.; Ditchfield, R.; Pople, J. A. *J. Chem. Phys.* **1972**, *65*, 2257.
(27) Fock, V. Z. *Physik* **1930**, *61*, 126.
(28) Curtis, L. A.; Raghavachari, K.; Trucks, G. W.; Pople, J. A., *J. Chem. Phys.* **1991**, *94*, 7221.
(29) Pople, J. A.; Head-Gordon, M.; Raghavachari, K. *J. Chem. Phys.* **1987**, *87*, 5968.
(30) Krishnan, R.; Binkley, J. S.; Seeger, R.; Pople, J. A. *J. Chem. Phys.* **1980**, *72*, 6.
(31) Becke, A. D. *J. Chem. Phys.* **1993**, *98*, 5648.
(32) Lee, C.; Yang, W.; Parr, R. G. *Phys. Rev. B* **1988**, *37*, 785.
(33) Frisch, M. J.; Trucks, G. W.; Schlegel, H. B.; Gill, P. M. W.; Johnson, B. G.; Robb, M. A.; Cheeseman, J. R.; Keith, T. A.; Petersson, G. A.; Montgomery, J. A.; Raghavachari, K.; Al-Laham, M. A.; Zakrezewski, V. G.; Ortiz, J. V.; Foresman, J. B.; Cioslowski, J.; Stefanov, B. B.; Nanayakkara, A.; Challacombe, M.; Peng, C. Y.; Ayala, P. Y.; Chen, W.; Fox, D. J.; Binkley, J. S.; Defrees, D. J.; Baker, J.; Stewart, J. P.; Head-Gordon, M.; Gonzales, C.; Pople, J. A. *Gaussian 94;* Gaussian, Inc.: Pittsburgh, PA, 1995.